First Principles Study of Mechanical Stability and Thermodynamic Properties of K_2S under Pressure and Temperature Effect

F. Boufadi[a], K. Bidai[a], M. Ameri[a,*], A. Bentouaf[a,b], D. Bensaid[a], Y. Azzaz[a] and I. Ameri[c]

[a]Laboratory of Physical Chemistry of Advanced Materials, University of Djillali Liabes, PO Box 89, Sidi-Bel-Abbes 22000, Algeria

[b]Hassiba Ben Bouali University, Faculty of Sciences, Department of Physics, 02000 Chlef, Algeria

[c]Djillali Liabes University, Faculty of Exact Sciences, Department of Physics, PO Box 089, Sidi Bel Abbes, 22000, Algeria

(Received October 18, 2015)

First principles calculations on structural, elastic and thermodynamic properties of K_2S have been made using the full-potential augmented plane-waves plus local orbitals within density functional theory using generalized gradient approximation for exchange correlation potentials. The ground state lattice parameter, bulk moduli have been obtained. The second-order elastic constants, Young and shear modulus, Poisson ratio, have also been calculated. Calculated structural, elastic and other parameters are in good agreement with available data. The elastic constants and thermodynamic quantities under high pressure and temperature are also calculated and discussed.

DOI: 10.12693/APhysPolA.129.315

PACS/topics: 62.20.de, 81.40.Jj, 71.15.Ap, 62.20.dj

1. Introduction

At room temperature, K_2S can crystallize stably into antifluorite (anti-CaF_2) structure type [1, 2] (space group no. 225). This structure is antimorphous to the fluorites (CaF_2). The cations and anion sublattices of these crystals have different symmetry, and is known as the antifluorite type structure. These antifluorite type structure materials are found to exhibit fast ionic conduction and they have attracted considerable attention due to their technological usefulness, and also by other remarkable and interesting physical properties. The alkali metal chalcogenide K_2S are characterized by their high ionic conductivity [3–5] and they exhibit large electronic band gaps. Apart from being used in power sources, fuel cells, gas-detectors and ultraviolet space technology devices [6–8], these ionic compounds also play important role in the development of photocathode, in supporting catalytic reactions and enhancing oxidation of semiconductor surfaces [9–16], and therefore are ideal for theoretical and experimental studies.

In the K_2S compound, the metal atoms (K) are located at (1/4, 1/4, 1/4) and (3/4, 3/4, 3/4) and the atoms (S) are located at (0, 0, 0). These compounds have been the subject of many experimental [1, 17, 18] and theoretical works [19–22] investigations. Most of the studies on M_2S [M: Li, Na, K and Rb] compounds have been dedicated to study elastic properties [17, 18] and the structural phase transformation [23–25]. Schon et al. [26] implemented the linear combination of atomic orbitals Hartree–Fock (LCAO-HF) method to analyze high pressure structural phase transition of M_2S compounds. Self-consistent pseudopotential method, the LCAO-HF and tight-binding linear muffin-tin orbital (TB-LMTO) studies have been reported by Zhuravlev et al. [27], Azavant et al. [28], and Eithiraj et al. [29], respectively, for electronic band structure of alkali metal sulfides. As well, Khachai et al. [20] have calculated the elastic properties of the X_2S (X = Li, Na, K, and Rb) compounds, under pressure effect, using the full potential augmented plane wave plus local orbitals (FP APW+lo) method. Khachai et al. [30] reported structural, electronic and optical properties of group-IA sulfides with and without applied pressure by using FP-APW+lo method.

Recent experimental results show that K_2S undergo a sequence of structural phase transformations under pressure. K_2S is found to undergo first-order phase transition from antifluorite to distorted Ni2In-type structure at 6 GPa [25]. From the theoretical point of view, the ground state as well as high pressure phases of alkali-metal sulfides has been studied up to a pressure of 100 GPa using the Hartree–Fock and density-functional theory [26]. The electronic band structure of these materials at ambient conditions was discussed by Zhuravlev et al. [27] using the self-consistent pseudopotential method.

To the best of our knowledge, there is a real lack of knowledge of their elastic properties, and thermodynam-

*corresponding author; e-mail: lttnsameri@yahoo.fr

ics properties of K_2S under pressure and temperature up to now. This lack has prompted us to investigate them. This work aims at presenting a first-principles study of the structure, elastic and thermodynamic properties under high pressures and temperatures of K_2S in the antifluorite phase, using full potential (linear) augmented plane wave plus local orbital (FP-APW+lo) method within the density functional theory based on the Perdew–Burke–Ernzerhof (PBE) functional. We describe the computational method used in this work in Sect. 2. The results are discussed in Sect. 3. Finally, a summary of the work is given in Sect. 4.

2. Computational methods

In the present paper, full-potential (linear) augmented plane wave plus local orbital (FP-APW+lo) method [31, 32] within the density functional theory (DFT) was used. This method has proven to be one of the most accurate methods for the computation of the electronic structure of solids within DFT [33–38], implemented in the WIEN2k code [39] has been applied for the study of structural, elastic, electronic, and thermodynamic properties of anti-CaF_2 structure type. Generalized gradient approximation based on the Perdew–Burke–Ernzerhof (PBE-GGA) functional [40, 41] has been used to determine the optimized structure of these compounds. In this method the unit cell is divided into non-overlapping spheres centered at atomic sites of radius and an interstitial region. APW+lo method expands the Kohn–Sham orbitals in atom-like muffin-tin spheres and plane waves in interstitial region. The basis set inside each muffin-tin sphere is split into core and valence subsets. The core states are treated within the spherical part of the potential only and are assumed to have a spherically symmetric charge density totally confined inside the muffin-tin spheres [31, 32, 42]. The valence part is treated within a potential expanded into spherical harmonics up to $l = 4$. The valence wave functions inside the spheres are expanded up to $l_{\max} = 10$. A plane-wave expansion with $R_{\mathrm{mt}}K_{\max} = 9$, and k sampling with a $8 \times 8 \times 8$ k-points mesh in the full Brillouin zone turns out to be satisfactory. The k integration over the Brillouin zone is performed using the Monkhorst and Pack mesh [43]. The energy that separates the valence state from the core state has been chosen to be –6.0 Ry. The leakage electrons from the muffin-tin radius are found to be less than 0.0001.

In order to obtain the thermodynamic properties of K_2S, the quasi-harmonic Debye model [44] is introduced, in which the non-equilibrium Gibbs function $G*(V,P,T)$ takes the form of

$$G^*(V,P,T) = E(V) + P(V) + A_{\mathrm{vib}}(\Theta(V),T). \quad (1)$$

In Eq. (1), $E(V)$ is the total energy for per unit cell of K_2S, PV corresponds to the constant hydrostatic pressure condition, $\Theta(V)$ is the Debye temperature as a function of V, and A_{vib} is the vibrational Helmholtz free energy which can be expressed as [45]:

$$A_{\mathrm{vib}}(\Theta,T) = nk_{\mathrm{B}}T\left[\frac{9\Theta}{8T} + 3\ln(1-\mathrm{e}^{-\Theta/T}) - D(\Theta/T)\right], \quad (2)$$

where $D(\Theta/T)$ is the Debye integral, and is defined as:

$$D(\Theta/T) = \frac{3}{(\Theta/T)^3}\int_0^{\Theta/T}\frac{x^3}{e^x-1}\,\mathrm{d}x, \quad (3)$$

where n represents the number of atoms per formula unit, Θ — the Debye temperature — is expressed as [45–47]:

$$\Theta = \frac{\hbar}{K}\left[6\pi^2V^{1/2}n\right]^{1/3} f(\sigma)\sqrt{\frac{B_{\mathrm{s}}}{M}}, \quad (4)$$

where M is the mass of per formula unit, σ is the Poisson ratio and B_{s} is the adiabatic bulk modulus that is approximated as

$$B_{\mathrm{s}} \cong B(V) = V\left(\frac{\mathrm{d}^2E(V)}{\mathrm{d}V^2}\right) \quad (5)$$

and the $f(\sigma)$ is given by

$$f(\sigma) = \left\{3\left[2\left(\frac{2(1+\sigma)}{3(1-2\sigma)}\right)^{3/2} + \left(\frac{1+\sigma}{3(1-\sigma)}\right)^{3/2}\right]^{-1}\right\}^{1-3}. \quad (6)$$

Therefore, for the given pressure P and temperature T with respect to the volume V, the non-equilibrium Gibbs function merely depends on $V(P,T)$ and can be solved as

$$\left(\frac{\partial G^*(V,P,T)}{\partial V}\right)_{P,T} = 0. \quad (7)$$

As a result, the isothermal bulk modulus B_T, the heat capacity C_V (at constant volume), the heat capacity C_P (at constant pressure), and the thermal expansion α are given by

$$B_T(P,T) = V\left(\frac{\partial^2G^*(V,P,T)}{\partial V^2}\right)_{P,T}, \quad (8)$$

$$C_V = 3nk_{\mathrm{B}}\left[4D(\Theta/T) - \frac{3\Theta/T}{\mathrm{e}^{\Theta/T}-1}\right], \quad (9)$$

$$C_p - C_V(1+\alpha\gamma T), \quad (10)$$

$$\alpha = \frac{\gamma C_V}{B_T V}. \quad (11)$$

The entropy is described by

$$S = nk_{\mathrm{B}}[4D(\Theta/T) - 3\ln(1-\mathrm{e}^{\Theta/T})], \quad (12)$$

where the Grüneisen parameter γ is defined as:

$$\gamma = -\frac{\mathrm{d}\ln\Theta(V)}{\mathrm{d}\ln V}. \quad (13)$$

3. Results and discussion

3.1. Structural properties

The total energies as a function of volume are fitted to Murnaghan's equation of states [48], to determine the ground state properties, such as equilibrium lattice parameter (a_0), total energies (E_0), bulk modulus (B_0) and its pressure derivatives (B_0') is presented in Fig. 1 for K_2S. Calculated ground state lattice parameter (a_0),

bulk modulus (b_0) and its first order pressure derivative (B_0'), obtained using GGA approximation are shown in Table I. The agreement between our calculated results for lattice constant for K_2S using GGA with the experimental data is reasonably good. When we analyse these results of B_0 and B_0', we find there is a good agreement between our results. All these properties along with the calculated values of elastic constants (C_{11}, C_{12} and C_{44}) in antifluorite phase for K_2S are presented in Tables I, II and compared with available theoretical and experimental results.

TABLE I

Calculated lattice constant a_0 (Å), bulk modulus B_0 (GPa), its first pressure derivatives B_0' for K_2S, compared to the experimental data and previous theoretical calculations.

	Parameters	Present work	Other calculations	Exp.
K_2S	a_0	7.468	7.475^t 7.193^t 7.387^n 7.626^p 6.981^p 7.066^p 7.779^p 7.341^m 7.387^f 7.198^l 7.480^l	7.391^a
	B_0	18.2159	19.03^t 23.70^t 27.29^n 29.41^p 28.67^p 26.09^p 21.48^p 27^c 25.9^d 31.0^e 18.9869^m 27.29^f 23.76^l 19.67^l	–
	B_0'	4.2877	3.85^l 3.72^l	–

^{a}Ref. [1]. ^{t}Ref. [30]. ^{n,f}Ref. [29]. ^{p}Ref. [26]. ^{l}Ref. [19]. ^{c}Ref. [61]. ^{d}Ref. [62]. ^{e}Ref. [63] ^{m}Ref. [64].

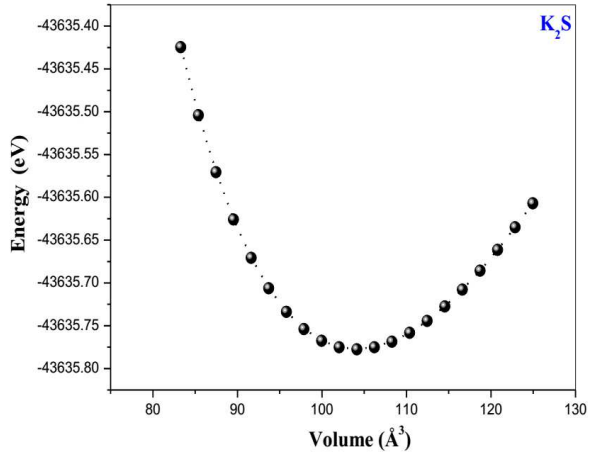

Fig. 1. Total energy as a function of volume for K_2S with GGA calculation.

3.2. Thermodynamic properties

The thermodynamic properties are studied over a range of pressures from 0 to 100 GPa and the temperature up to 1000 K. The temperature effect on the volume of K_2S compound is documented in Fig. 2. It can be seen that the volume increases linearly with increasing temperature. The rate of increase is almost zero from $T = 0$ to 100 K and becomes very moderate for $T > 100$ K. On the other side, as the pressure increases, the volume decreases at a given temperature. Generally speaking, the volume increases as the temperature increases, and decreases as the pressure increases. The calculated equilibrium primitive cell volume V at zero pressure and room temperature is 105.11 Å^3. The relationship between the bulk modulus B and temperature at different pressures is shown in Fig. 3. These results indicate that B decreases with T at a given pressure and increases with P at a given temperature. It shows the fact that the effect of increasing pressure on K_2S is the same as decreasing its temperature.

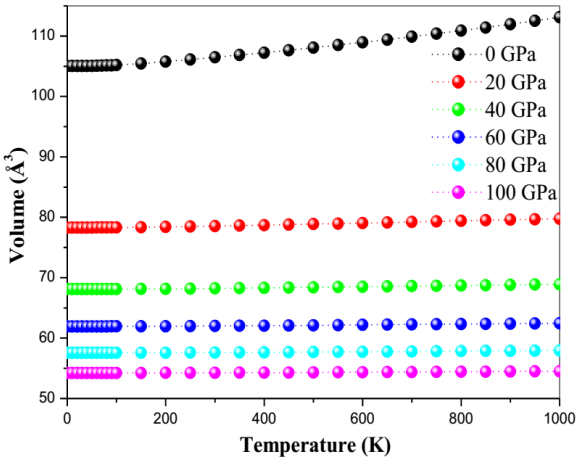

Fig. 2. The variation of the primitive cell volume as a function of temperature at different pressures of K_2S.

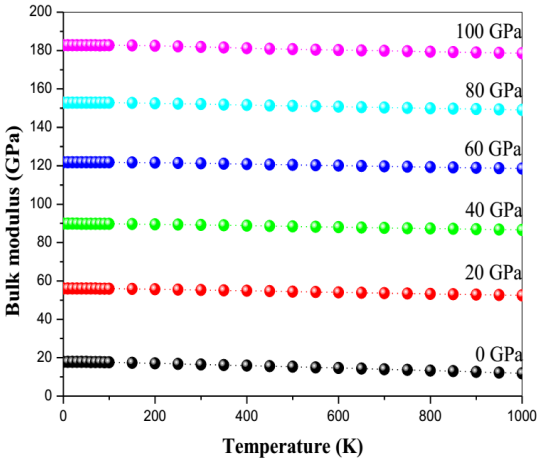

Fig. 3. Temperature dependence of bulk modulus B of K_2S at different pressure.

The heat capacity is an important parameter of the condensed matter physics. It does not only provide a fundamental insight into their vibrational properties but is also mandatory for many applications. At intermediate temperatures, temperature dependence of the heat capacity C_V is governed by the details of the vibrations of atoms and has been able to be determined only

experimentally for a long time past [49]. Figures 4 and 5 show the calculated specific heats at constant volume C_V and constant pressure C_P of K_2S. At low temperatures, the shapes of curves of C_V and C_P are similar. The data of C_V and C_P are proportional to T^3. At higher temperatures, C_V becomes close to the Dulong–Petit limit; when $T > 800$ K, and C_P deviates from C_V and trends to be linear with the temperature. Our calculated value of C_V at zero-pressure and at 300 K is 70.226 for K_2S.

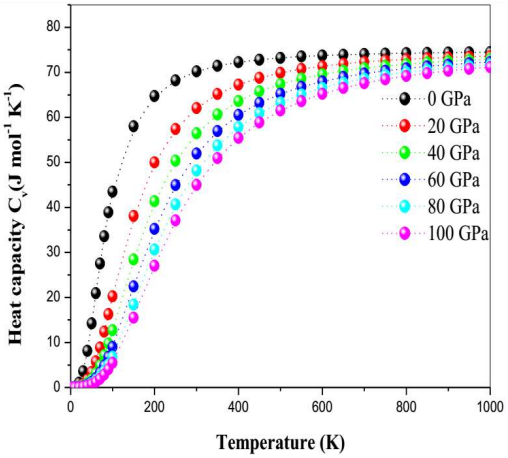

Fig. 4. Calculated temperature dependence of heat capacity of K_2S at constant volume (C_V).

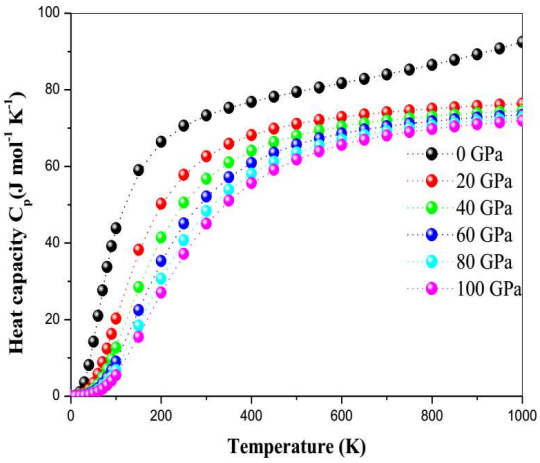

Fig. 5. Temperature dependence of heat capacity of K_2S at constant pressure (C_P).

In Fig. 6, we present the effect of the temperature and pressure on the thermal expansion α. It is shown that the thermal expansion coefficient increases with increasing temperature. For a given temperature, the thermal coefficient α decreases sharply with increasing pressure and becomes smaller at higher temperatures and pressures. For a given pressure, α increases sharply with the increase of temperature up to 200 K. Above this temperature, α gradually approaches to a linear increase with enhanced temperature. At zero pressure and 300 K, the thermal expansion α is 7.03×10^{-5} K.

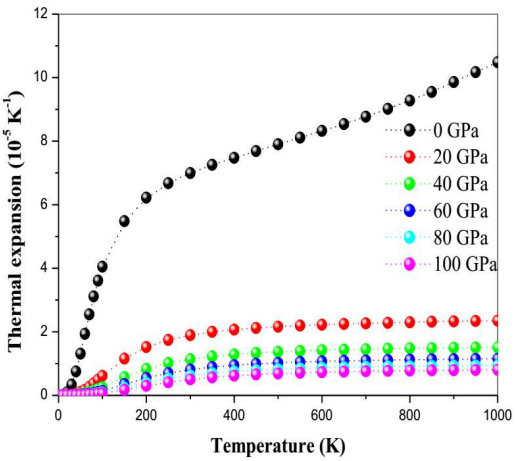

Fig. 6. Thermal expansion as a function of temperature (T) of K_2S at different pressure.

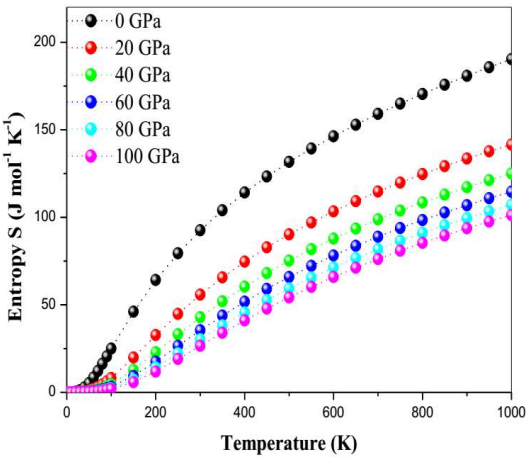

Fig. 7. The variation of the entropy as a function of temperature at different pressures of K_2S.

The entropy S under high pressure and high temperature can be obtained according to Eq. (12). Figure 7 shows the curve of entropy S at different pressure and temperature. The curves indicate that the entropy decreases with pressure at a given temperature and increases monotonously with temperature at a fixed pressure. It indicates that the effect of increasing pressure on K_2S is same as that of decreasing temperature.

The Debye temperature (Θ_D) is an important parameter characteristic for the thermal properties of solids. It is the temperature above which the crystal behaves classically, because the thermal vibrations become more important than the quantum effects. The variation of the Debye temperature as a function of pressure and temperature is plotted in Fig. 8. It can be seen from Fig. 8 that Θ_D is nearly constant from 0 to 100 K; above 100 K, Θ_D decreases linearly with increasing temperature. At fixed temperature, the Debye temperature increases with the increase in pressure. At zero pressure, Θ_D is lower than that at higher pressures.

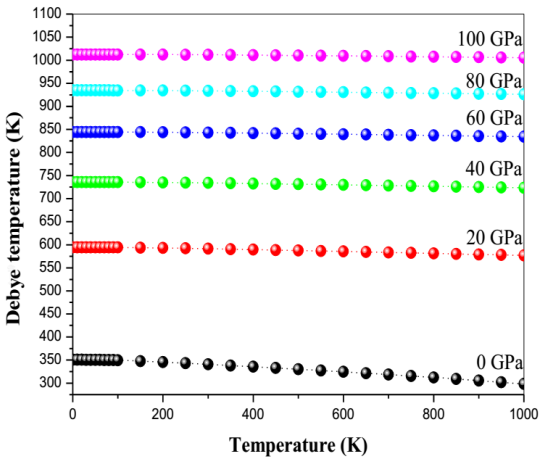

Fig. 8. The variation of the Debye temperature as a function of temperature at different pressures of K_2S.

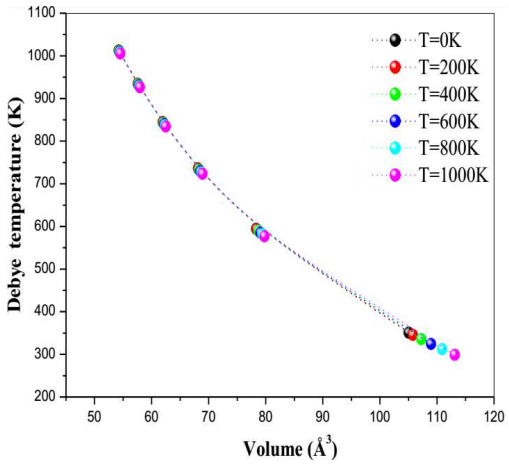

Fig. 9. The variation of the Debye temperature as a function of volume at different pressures of K_2S.

The Debye temperatures Θ_D of the K_2S compound at the temperature of 300 K are higher than those at 1000 K, as shows the fact that the vibration frequency of the particles in K chalcogens: K_2S changes with the pressures and the temperatures. The calculated value of the Debye temperatures Θ_D for K_2S at zero pressure and zero temperature is found to be equal to 350.08 K. The volume dependence of the Debye temperature Θ_D is shown in Fig. 9 at some fixed temperatures. All points lie on a single curve, demonstrating both the consistency of our calculations and the fact that the Debye temperature is a function of the volume only is the quasi-harmonic approximation which introduces the temperature dependence through the volume and the simplification given by Eq. (4). It is noted that as the volume V increases, the value of the Debye temperature decreases. The relatively small effect of the temperature on the Debye temperature can be explained by the small effect on the volume changes. It is observed that for constant temperature the Debye temperature of the herein studied materials increases almost linearly with the decrease of the volume.

3.3. Elastic properties

The elastic properties of solids are important because they are related to various fundamental solid state phenomena, such as interatomic potential, equation of state, phonon spectra. Elastic properties are also linked thermodynamically with specific heat, thermal expansion, the Debye temperature, melting point, and the Grüneisen parameter [50–52]. Most importantly, knowledge of the elastic constants is essential for many practical applications related to the mechanical properties of a solid: load deflection, thermoelastic stress, internal strain, sound velocities, and fracture toughness. In our case, the K_2S compound have a cubic symmetry; hence, only three independent elastic constants, C_{11}, C_{12}, and C_{44}, needed to be calculated. C_{ij} values were obtained through the Mehl method by calculating the total energy as a function of volume-conserving strains [49, 53]. We have calculated the elastic constants (C_{11}, C_{12}, C_{44}) for K_2S in their antifluorite phase.

TABLE II

Calculated elastic constants (in GPa) for K_2S in anti-CaF2 structure.

Material	Parameters	Present work GGA	Other calculations[a]
K_2S	C_{11}	33.99	GGA (LDA) 34.58 40.01
	C_{12}	10.33	GGA (LDA) 10.71 15.63
	C_{44}	11.80	GGA (LDA) 11.85 12.11

[a]Ref. [19].

TABLE III

Calculated Zener anisotropy factor A, Poisson's ratio ν, bulk modulus B (in GPa), shear modulus G (in GPa), Young's modulus E (in GPa).

Material		B	G	E	A	B/G	ν
K_2S	present work: GGA	18.22	11.81	29.14	0.99	1.54	0.23
	other calc.[a]:						
	GGA	19.67	11.88	29.41	–	–	0.23
	LDA	23.76	12.14	31.12	–	–	0.28

[a]Ref. [19].

Elastic moduli of K_2S obtained from energy variations due to application of small strain to equilibrium lattice configuration, have been given in Table II. The calculations of the elastic constants are very significant to understand and give information about the stability of our material. We determine the elastic constants which are related to the bulk modulus B, Young's modulus E, isotropic shear modulus G and Poisson's ratio have also been listed in Table III. To the best of our knowledge, no experimental values of elastic moduli for the studied compound are available in literature. The mechanical [54, 55] ($C_{11} + 2C_{12} > 0$, $C_{11} - C_{12} > 0$, $C_{44} > 0$, $C_{11} > 0$) can lead for the validity of elastic moduli. The calculated

elastic constant values satisfy all these stability conditions, including the fact that $C_{12} > C_{11}$. Furthermore, calculated elastic moduli also satisfy the cubic stability condition i.e. $C_{12} < B < C_{11}$.

The Zener anisotropy factor (A) is an indicator of the degree of anisotropy in the solid structures. For a completely isotropic material, the A factor takes the value of 1, when the value of A is smaller or greater than unity it is a measure of the degree of elastic anisotropy. Poisson's ratio (ν), shear modulus (G), and Young's modulus (E), which are the most interesting elastic properties for applications, are often measured for polycrystalline materials when their hardness has been investigated. These quantities are calculated in terms of the computed data using the following relations [56]:

$$A = \frac{2C_{44}}{C_{11} - C_{12}}, \tag{14}$$

$$\nu = \frac{3B - 2G}{6B + 2G}, \tag{15}$$

and

$$E = \frac{9BG}{3B + G}, \tag{16}$$

where $G = (G_{\mathrm{V}} + G_{\mathrm{R}})/2$ is the isotropic shear modulus, G_{V} is Voigt's shear modulus corresponding to the upper bound of G values, and G_{R} is Reuss'es shear modulus corresponding to the lower bound of G values, and can be written as [57]:

$$G_{\mathrm{V}} = \frac{C_{11} - C_{12} + 3C_{44}}{5}, \tag{17}$$

and

$$G_{\mathrm{R}} = \frac{5(C_{11} - C_{12})C_{44}}{4C_{44} + 3(C_{11} - C_{12}}. \tag{18}$$

The calculated Zener anisotropy factor (A), Poisson's ratio (ν), Young's modulus (E), and shear modulus G are summarised in Table III. The calculated elastic constants (C_{11}, C_{12}, C_{44}) are in good agreement with the predictions of other computational method [19].

Calculated A values for K_2S under ambient temperature and pressure are 0.99 which are approach than 1 considered as isotropic (Table III).

The value of the Poisson ratio (ν) for covalent materials is small (= 0.1), whereas for ionic materials a typical value is 0.25 [58]. In our case the value of ν is 0.23, i.e. a higher ionic contribution in intra-atomic bonding for this compound should be assumed.

The bulk modulus B represents the resistance to fracture [59], while the shear modulus G represents the resistance to plastic deformation [60]. A high Pugh B/G ratio is associated with ductility, whereas a low value corresponds to the brittle nature. The critical value which separates ductile and brittle material is 1.75; i.e., if $B/G > 1.75$, the material behaves in a ductile manner; otherwise the material behaves in a brittle manner [29]. Now we have found that the B/G ratio is 1.54 for this compound, classifying K_2S as brittle.

Now we are studying the pressure dependence of the elastic properties. In Fig. 10, we present the variation

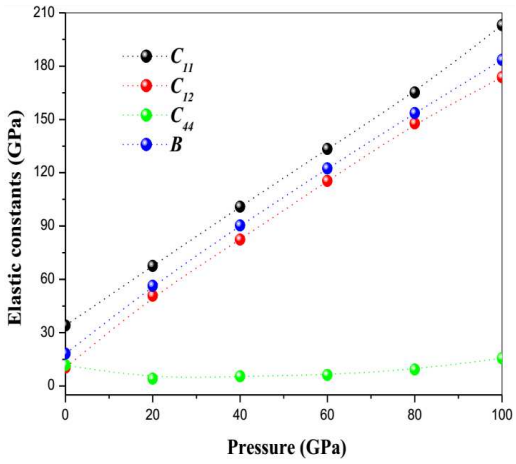

Fig. 10. Pressure dependence of the elastic constants (C_{11}, C_{12} and C_{44}) and B of K_2S.

of the elastic constants and bulk modulus for this compound with respect to the variation of pressure. It is easy to observe that all the elastic constants and the bulk modulus increase when the pressure is increased. C_{11} and C_{12} are more sensitive to the change of pressure compared to C_{44}. In order to study the temperature dependence of the elastic properties of these compounds, we have focused our study on the temperature range from 0 to 1000 K.

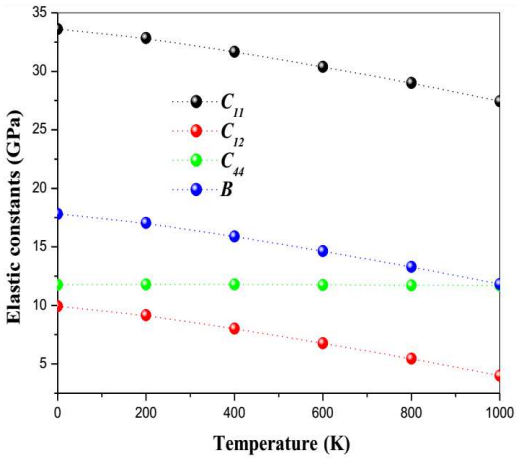

Fig. 11. Temperature dependence of the elastic constants (C_{11}, C_{12} and C_{44}) and B of K_2S.

The temperature variations of the isothermal elastic constants C_{ij}^{T} for K_2X compounds are presented in Fig. 11. We clearly observe that the elastic constants: C_{11}^{T}, C_{12}^{T}, and C_{44}^{T} increase when the temperature is enhanced. In particular, we have found a small linear increase for C_{44}^{T}. However, the variation of C_{11}^{T} and C_{12}^{T} with temperature is found to be larger as compared with C_{44}^{T}. These later are related to the elasticity in shape which is shear constant. It is known that a

longitudinal strain produces a change in volume without a change in shape, and from above we have seen that the volume change is highly related to the temperature and thus produces a large change in C_{11}^{T} and C_{12}^{T}. On the other hand, a transverse strain or shearing causes a change in shape without a change in volume. Thus, C_{44}^{T} are less sensitive of temperature.

4. Conclusion

First principles method has been used to study the structural, elastic, electronic and thermodynamic properties of K_2S in the antifluorite structure. The following conclusions have been drawn from the calculations. Calculations indicate that the present values of equilibrium lattice constant, a_0 and bulk moduli, B_0 are in good agreement with available literature values. The present calculations provide reliable values of elastic moduli at absolute zero temperature and zero pressure of K_2S with the accuracy of the PBE-GGA exchange-correlation functional. Young's modulus, shear modulus, Poisson's ratio, and other elastic properties have also been calculated for these compound at ambient pressure. We have also calculated and presented the thermodynamic quantities, elastic constants C_{ij} under high pressure and temperature.

References

[1] E. Zintle, A. Harder, B. Dauth, *Z. Electrochem.* **40**, 588 (1934).

[2] J. Sangster, A.D. Pelton, *J. Phase Equilib.* **18**, 190 (1997).

[3] W. Bührer, H. Bill, *J. Phys. C Solid State Phys.* **13**, 5495 (1980).

[4] P.M. Mjwara, J.D. Comins, P.E. Ngoepe, W. Bührer, H. Bill, *J. Phys. Condens. Matter* **3**, 4289 (1991).

[5] H. Kikuchi, H. Iyetomi, A. Hasegawa, *J. Phys. Condens. Matter* **10**, 11439 (1989).

[6] D. Biseri, A. di Bona, P. Paradisi, S. Valeri, *J. Appl. Phys.* **87**, 543 (2000).

[7] A. Piccioli, R. Pegna, I. Fedorko, M. Giunta, N. Malakhov, *Nucl. Instrum. Methods Phys. Res. A* **518**, 602 (2004).

[8] C. Joram, *Nucl. Phys. B* **78**, 407-415 (1999).

[9] T. Minami, A. Hayashi, M. Tatsumisago, *Solid State Ionics* **136–137**, 1015 (2000).

[10] J.S. Esher, *Semiconductors and Semimetals*, Academic Press, New York 1981, p. 195.

[11] C. Gosh, *Phys. Thin Films Photoemissive Mater.* **12**, 75 (1982).

[12] D. Bisero, B.M. van Oerle, G.J. Ernst, J.W.J. Verschuur, W.J. Witteman, *Appl. Phys. Lett.* **69**, 3641 (1996).

[13] D. Bisero, B.M. van Oerle, G.J. Ernst, J.W.J. Verschuur, W.J. Witteman, *J. Appl. Phys.* **82**, 1384 (1997).

[14] C.T. Campbell, *J. Catal.* **94**, 436 (1985).

[15] P. Soukiassian, H.I. Starnberg, in: *Physics and Chemistry of Alkali Metal Adsorption*, Eds. H.P. Bonzel, A.M. Bradshaw, G. Ertl, Elsevier, Amsterdam 1989, p. 449.

[16] S. Hull, T.W.D. Farley, W. Hayes, M.T. Hutchings, *J. Nucl. Mater.* **160**, 125 (1988).

[17] W. Bührer, H. Bill, *Helv. Phys. Acta* **50**, 431 (1977).

[18] W. Bührer, F. Altorfer, J. Mesot, H. Bill, P. Carron, H.J. Smith, *J. Phys. Condens. Matter.* **3**, 1055 (1991).

[19] H. Khachai, R. Khenata, A. Bouhemadou, A.H. Reshak, A. Haddou, M. Rabah, B. Soudini, *Solid State Commun.* **147**, 178 (2008).

[20] S.M. Alay-e-Abbas, N. Sabir, Y. Saeed, A. Shaukat, *Int. J. Mod. Phys. B* **25**, 3911 (2011).

[21] S.M. Alay-e-Abbas, A. Shaukat, *J. Mater. Sci.* **46**, 1027 (2011).

[22] R.D. Eithiraj, G. Jaiganesh, G. Kalpana, *Int. J. Mod. Phys. B* **23**, 5027 (2009).

[23] A. Grzechnik, A. Vegas, K. Syassen, L. Loa, M. Hanfland, M. Jansen, *J. Solid State Chem.* **154**, 603 (2000).

[24] A. Vegas, A. Grzechnik, K. Syassen, L. Loa, M. Hanfland, M. Jansen, *Acta Crystallogr. B* **57**, 151 (2001).

[25] A. Vegas, A. Grzechnik, M. Hanfland, C. Muhle, M. Jansen, *Solid State Sci.* **4**, 1077 (2002).

[26] J.C. Schon, Z. Cancarevic, M. Jansen, *J. Chem. Phys.* **121**, 2289 (2004).

[27] Y.N. Zhuravlev, A.B. Kosobutskii, A.S. Poplavnoi, *Russ. Phys. J.* **48**, 138 (2005).

[28] P. Azavant, A. Lichanot, M. Rérat, *Acta Crystallogr. B* **50**, 279 (1994).

[29] R.D. Eithiraj, G. Jaiganesh, G. Kalpana, M. Rajagopalan, *Phys. Status Solidi B* **244**, 1337 (2007).

[30] H. Khachai, R. Khenata, A. Bouhemadou, A. Haddou *J. Phys. Condens. Matter* **21**, 095404 (2009).

[31] G.K.H. Madsen, P. Blaha, K. Schwarz, E. Sjöstedt, *Phys. Rev. B* **64**, 195134 (2001).

[32] K. Schwarz, P. Blaha, G.K.H. Madsen, *Comput. Phys. Commun.* **147**, 71 (2002).

[33] A.H. Reshak, S. Auluck, I.V. Kityk, *J. Phys. D Appl. Phys.* **42**, 085406 (2009).

[34] A.H. Reshak, X. Chen, F. Song, I.V. Kityk, S. Auluck, *J. Phys. Condens. Matter* **21**, 205402 (2009).

[35] A.H. Reshak, S. Auluck, I.V. Kityk, *J. Phys. Chem. A* **113**, 1614 (2009).

[36] A.H. Reshak, I.V. Kityk, S. Auluck, *J. Phys. Chem. B* **114**, 16705 (2010).

[37] A.H. Reshak, S. Auluck, D. Stys, I.V. Kityk, H. Kamarudin, J. Berdowski, Z. Tylczynski, *J. Mater. Chem.* **21**, 17219 (2011).

[38] A.H. Reshak, H. Kamarudin, S. Auluck, B. Minofar, I.V. Kityk, *Appl. Phys. Lett.* **98**, 201903 (2011).

[39] P. Blaha, K. Schwarz, G.K.H. Madsen, D. Kvasnicka, J. Luitz, WIEN2k (2001), University of Technology, Vienna, Austria, *An Augmented Plane Wave Plus Local Orbitals Program for Calculating Crystal Properties*, www.wien2k.at; P. Blaha, K. Schwarz, P. Sorantin, S.B. Trickey, *Comput. Phys. Commun.* **59**, 399 (1990).

[40] J.P. Perdew, Y. Wang, *Phys. Rev. B* **45**, 13244 (1992).

[41] P. Perdew, S. Burke, M. Ernzerhof, *Phys. Rev. Lett.* **77**, 3865 (1996).

[42] E. Sjostedt, L. Nordstrom, D. Singh, *J. Solid State Commun.* **114**, 15 (2000).

[43] H.J. Monkhorst, J.D. Pack, *Phys. Rev. B* **13**, 5188 (1976).

[44] A.A. Maradudin, E.W. Montroll, G.H. Weiss, I.P. Ipatova, *Theory of Lattice Dynamics in the Harmonic Approximation*, Academic Press, New York 1971.

[45] M.A. Blanco, E. Francisco, V. Luaña, *Comput. Phys. Commun.* **158**, 57 (2004).

[46] M.A. Blanco, A. Martin Pendas, E. Francisco, J.M. Recio, R. Franco, *J. Mol. Struct. Theochem.* **368**, 245 (1996).

[47] M. Florez, J.M. Recio, E. Francisco, M.A. Blanco, A. Martin Pendas, *Phys. Rev. B* **66**, 144112 (2002).

[48] F.D. Murnaghan, *Proc. Natl. Acad. Sci.* **30**, 244 (1944).

[49] M.J. Mehl, *Phys. Rev. B* **47**, 2493 (1993).

[50] R.G. Leissure, K. Foster, J.E. Hightower, D.S. Agosta, *J. Alloys Comp.* **356**, 283 (2003).

[51] P. Rvindran, L. Fast, P.A. Korzhavyi, B. Johansen, *J. Appl. Phys.* **84**, 4891 (1998).

[52] V. Kanchana, G. Vaitheeswaran, A. Svane, A. Delin, *J. Phys. Condens. Matter* **18**, 9615 (2006).

[53] E. Schreiber, O.L. Anderson, N. Soga, *Elastic Constants and Their Measurements*, McGraw-Hill, New York 1973.

[54] A. Bouhemadou, R. Khanate, M. Kharoubi, T. Seddik, A.H. Reshak, Y.A. Douri, *Comput. Mater. Sci.* **45**, 474 (2009).

[55] D. Heciri, L. Beldi, S. Drablia, H. Meradji, N.E. Derreadji, H. Belkhir, B. Bouhafs, *Comput. Mater. Sci.* **38**, 609 (2007).

[56] B. Mayer, H. Anton, E. Bott, M. Methfessel, J. Sticht, P.C. Schmidt, *Intermetallics* **11**, 23 (2003).

[57] M. Mattesini, R. Ahuja, B. Johansson, *Phys. Rev. B* **68**, 184108 (2003).

[58] J. Haines, J.M. Leger, G. Bocquillon, *Annu. Rev. Mater. Res.* **31**, 1 (2001).

[59] G. Vaitheeswaran, V. Kanchana, R.S. Kumar, A.L. Cornelius, M.F. Nicol, A. Savane, A. Delin, B. Johansson, *Phys. Rev. B* **76**, 014107 (2007).

[60] S.F. Pugh, *Philos. Mag.* **45**, 823 (1954).

[61] S.D. Chaturvedi, S.B. Sharma, P.Paliwal, M Kumar., *Phys. Status Solidi B* **156**, 171 (1989).

[62] V.K. Jain, J. Shanker, *Phys. Status Solidi B* **114**, 287 (1982).

[63] A. Melillou, B.R.K. Gupta, *J. Phys.* **41**, 813 (1991).